USP10-mediated ZEB1 deubiquitination regulates MEK-ERK-induced colorectal cancer metastasis

Frank Sinicrope (sinicrope.frank@mayo.edu)
Mayo Clinic https://orcid.org/0000-0002-2907-1000
Bo Qin
Mayo Clinic https://orcid.org/0000-0001-8993-240X
Lei Sun
Jia yu

Article

Keywords:

Posted Date: June 15th, 2022

DOI: https://doi.org/10.21203/rs.3.rs-1735411/v1

Abstract

Zinc finger E-box binding homeobox 1 (ZEB1) is a transcription factor regulating epithelial to mesenchymal transition (EMT). To date, regulation of ZEB1 by key signaling pathways including RAS/RAF/MEK/ERK remains unclear, and few studies have focused on molecular associations or functional alterations of ZEB1 by post-translational modification. Here, we report an interaction of ZEB1 with the deubiquitinase USP10 that is regulated by MEK-ERK signaling. USP10 removes the K27 linkage ubiquitination chain on ZEB1 that enhances K48 polyubiquitination and promotes ZEB1 proteasomal degradation. However, constitutive activation of ERK can phosphorylate USP10 at Ser^{236} to impair its interaction with ZEB1 and, thereby, stabilize ZEB1 protein shown to promote colorectal cancer metastasis in mice. Conversely, inhibition of MEK-ERK blocks USP10 phosphorylation to enhance the USP10-ZEB1 interaction which can suppress ZEB1-mediated tumor cell migration and metastasis *in vivo*. Together, these data demonstrate a novel function of USP10 in the regulation of ZEB1 ubiquitination and protein stability that can inhibit ZEB1-mediated tumor metastasis.

Introduction

Colorectal cancer (CRC) is the 3rd most common cancer in the U.S. and is 2nd only to lung cancer as a cause of cancer-related mortality [1]. Of new cases of CRC, 20% of patients have metastatic disease and another 25% who present with localized disease will later develop metastases [2]. Elucidating the molecular mechanisms underlying tumor metastasis is essential for the development of therapeutic strategies against CRC. Tumor metastasis is mediated by epithelial-to-mesenchymal transition (EMT) and this phenotype is associated with invasion, tumor progression and metastasis[3]. With EMT, cells lose their epithelial characteristics and gain mesenchymal properties such as increased cell migration, tissue remodeling/wound repair and enhanced cancer stemness [4, 5]. Pleiotropic transcription factors including the double zinc finger and homeodomain factor, ZEB1, regulate EMT and ZEB1 promotes tumor metastasis and treatment resistance in multiple cancer cell types, including CRC [6, 7]. ZEB1 can repress the expression of epithelial and pro-metastatic genes, such as E-cadherin [8, 9], and its overexpression in human CRCs is associated with poorer prognosis compared to tumors with low or absent expression[10].

The ZEB1 protein is subject to ubiquitination and degradation, although the mechanism by which ZEB1 is stabilized in cancer cells is largely unknown [11, 12]. Ubiquitination is a posttranslational modification that regulates many cellular processes through protein stability, activity or localization [13]. Ubiquitin has seven lysine residues (K6, K11, K27, K29, K33, K48, K63) and an N-terminus (M1) which can be conjugated by other ubiquitin moieties to form a polyubiquitination chain [14]. Lysine 48-linked chains target substrate proteins for proteasomal degradation while the function of K27-linked ubiquitination is poorly understood. Ubiquitination can be reversed by deubiquitinase (DUB) that regulate protein stability of which only three DUBs have been shown to remove K27-linkange polyubiquitination chains from their substrates [15–17]. In this study, we sought to find a DUB(s) that may interact with ZEB1 and identified a ubiquitin-specific protease 10 (USP10) as a potential candidate. USP10 is ubiquitously expressed in many cancer cell types [18], and has been shown to stabilize p53 and SIRT6 proteins as well as the

NOTCH1 intracellular domain [19, 20, 21]. Previously, we found that USP10 can remove the K63-linkage polyubiquitination chain on AMPKα and facilitate AMPKα phosphorylation by LKB1 [22]. USP10 has also been reported to remove the K63 linkage chain from PTEN which restored PTEN phosphatase activity [23].

In this study, we determined whether the DUB USP10 could regulate ZEB1 stability in human CRC cells that may contribute to its role in tumor metastasis. We found that ZEB1 could be stabilized by MEK-ERK signaling and demonstrated for the first time that USP10 could remove the K27 linkage polyubiquitination chain from ZEB1 which enhanced K48 polyubiquitination of ZEB1 and promoted its proteasomal degradation. These events were shown to suppress the EMT processes of tumor cell migration and metastasis in a mouse xenograft model.

Results

ZEB1 protein stability is regulated by MEK-ERK signaling

We examined the expression of protein products of EMT transcription factors in CRC cell lines with constitutive MEK-ERK activation. In RKO isogenic cell lines expressing *BRAF*^{V600E} vs *BRAF* wild-type (wt) [T29], only ZEB1 and ZEB2 protein levels were increased (Fig.1A-B). Treatment of these cells with the MEK inhibitor cobimetinib suppressed expression of ZEB1 but not ZEB2 (Fig.1B). Similarly, treatment of RKO cells with the selective *BRAF*^{V600E} inhibitors vemurafenib (Fig.1C) or encorafenib (Fig. 1D) were each shown to suppress ZEB1 expression. Furthermore, another MEK inhibitor trametinib was also shown to decrease ZEB1 expression (Fig. 1D). In Colo320 cells transfected with a mutant *KRAS* G12D plasmid, induction of ZEB1 protein expression was observed (Fig.1E). Among EMT factors, these data demonstrate preferential regulation of ZEB1 by MEK-ERK signaling.

Treatment of RKO isogenic cells with the proteasome inhibitor, MG132, enhanced ZEB1 expression in *BRAF*^{V600E} and in wt cell lines (Fig.1F) indicating that ZEB1 undergoes proteasomal degradation. Cells treated with MG132 showed decreased K48-linkage polyubiquitinated ZEB1 protein in *BRAF*^{V600E} cell in contrast to wt cells (Fig.1G), and this ubiquitination could be reversed by MEK inhibitor treatment (Fig.1H). Enhanced ZEB1 stability was also observed in *BRAF*^{V600E} compared to *BRAF* wt cells by treating RKO isogenic cells with an inhibitor of protein synthesis, i.e., cycloheximide (Fig. 1D). Treatment with cobimetinib increased proteasomal degradation of ZEB1 (Fig.1J). Together, these results suggest that MEK-ERK activation can protect ZEB1 from proteasomal degradation to enhance its stability.

The functional consequence of ZEB1 stabilization was examined in a wound healing assay. Isogenic *BRAF*^{V600E} cells with overexpression of ZEB1 were observed to migrate faster than did cells with *BRAF wt* (Fig.1K), and this result was confirmed in a transwell assay (Fig.1L-M). An inhibitor of MEK, shown to suppress ZEB1 (Fig. 1B), blocked CRC cell migration (Fig.1N-P). These data suggest that regulation of ZEB1 stability by MEK-ERK can modulate CRC cell migration.

USP10 can destabilize ZEB1 protein

Deubiquitinases (DUBs) can regulate protein stability and in a prior study, we reported that ubiquitin-specific protease 10 (USP10) could deubiquitinate and thereby activated AMPK [22]. We examined the BioGrid database to identify potential DUBs that may interact with ZEB1 and identified USP10 as a potential candidate (supplementary table S1). As shown in Fig.2A-B, USP10 co-immunoprecipitated with ZEB1 in RKO cells. For confirmation, reciprocal immunoprecipitation using antibodies against USP10 or ZEB1 were shown to pull down ZEB1 or USP10 proteins, respectively, in Colo320 cells (Fig.2C-D). Since USP10 is a ubiquitin-specific protease, we determined if USP10 can stabilize ZEB1. Unexpectedly, knockdown of *USP10* in RKO cells significantly increased the level of endogenous ZEB1 protein (Fig.2E). USP10 knockdown using a second shRNA was also shown to induce ZEB1 (Fig.2E), and consistent results were observed in Colo320 cells (Fig.2F). To determine whether USP10 can regulate ZEB1 stability, we treated cells expressing *USP10* shRNA or control shRNA with cycloheximide and observed that ZEB1 induction was due to its enhanced stability in *USP10* knockdown cells (Fig.2G). Furthermore, we found that K48-linkage polyubiquitination of ZEB1 was decreased in cells expressing *USP10* shRNA (Fig.2H), indicating impaired proteasomal degradation. Together, these results suggest that USP10 serves to destabilize ZEB1 in human CRC cells.

Since depletion of *USP10* can induce ZEB1, we then determined the effect of USP10 on the ability of ZEB1 to regulate CRC cell migration. Using a wound healing assay and a transwell assay, we found that knockdown of *USP10* and its associated induction of ZEB1 (Fig. 2E,F), can enhance cell migration in both assays (Fig.2I-K). To further confirm that USP10 regulates cell migration through ZEB1, we performed a knockdown of *USP10* or *ZEB1* separately or together. CRC cells expressing *USP10* shRNA showed faster migration whereas as cells with *ZEB1* shRNA displayed slower migration (Fig. 2L). Knockdown of *USP10* in cells with *ZEB1* shRNA did not accelerate cell migration (Fig.2L), indicating that USP10 regulates cell migration through ZEB1.

Activated MEK-ERK signaling promotes cell migration through USP10

We demonstrated that ZEB1 induction was due to its enhanced stability in *USP10* knockdown cells (Fig. 2G). To determine if ERK signaling can mediate stabilization of ZEB1 through USP10, knockdown of *USP10* in isogenic cells increased ZEB1 expression in *BRAF* mutant vs wildtype cells to a similar level (Fig.3A) that was associated with decreased K48 ubiquitination of ZEB1 (Fig.3B). The functional consequence of this finding was shown in a wound healing assay and a transwell assay that examined cell migration. In RKO and T29 cells with control shRNA expression, RKO cells expressing $BRAF^{V600E}$ migrated faster than did T29 cells. However, knockdown of *USP10* in both cell lines was shown to increase cell migration to a similar extent (Fig. 3C). In a transwell assay, depletion of *USP10* was also shown to enhance migration of both isogenic CRC cell lines (Fig.3 D,E). Taken together, activation of MEK-ERK can stabilize ZEB1 and promote cell migration through USP10.

We then inhibited ERK signaling which was shown to suppress ZEB1 and its regulation by USP10. In RKO and Colo320 cells treated with cobimetinib, we observed a decrease in ZEB1 protein level compared to control treated cells (Fig.4 A,B). Knockdown of *USP10* increased ZEB1 expression in the presence or absence of a MEK inhibitor (Fig.4 A,B) or the BRAF inhibitor, vemurafenib (Fig.4C). Enhanced K48 ubiquitination of ZEB1 was detected in both cobimetinib and vemurafenib treated cells, but knockdown of *USP10* impaired these ubiquitination signals (Fig.4D-E). Cobimetinib was shown to suppress CRC cell migration whereas depletion of *USP10* reversed and accelerated cell migration even in the presence of MEK inhibition (Fig.4F-H). Accordingly, suppression of MEK-ERK can destabilize ZEB1 through USP10.

USP10 destabilizes ZEB1 by editing its ubiquitination

As a DUB, USP10 can stabilize its substrate or regulate substrate activity. To elucidate the mechanism of ZEB1 protein destabilization by USP10, we transfected control and *USP10* depleted RKO cells with a panel of ubiquitin mutants where only one lysine was intact. We detected ZEB1 ubiquitination with different lysine linkage. Unexpectedly, we found that K27- linkage ubiquitinated ZEB1 was decreased, whereas K48-linkage ubiquitinated ZEB1 was consistently increased in *USP10* knockdown cells (Fig.5A). This finding suggests that USP10 can selectively remove K27-linkage to allow for subsequent K48-linked ubiquitination of ZEB1. *USP10* knockdown was shown to increase K27 ubiquitination and inhibit K48 ubiquitination of ZEB1. To confirm this result, we re-introduced wildtype *USP10* or a catalytically dead mutant of *USP10* into *USP10* knockdown cells. Reconstitution of wildtype *USP10* was shown to reverse the ubiquitination pattern of ZEB1, but not cells with the catalytic dead mutant (Fig.5B).

To assess the functional consequence of regulation of ZEB1 by USP10, CRC cell migration was again analyzed. We observed increased cell migration in *USP10* knockdown cells in presence or absence of cobimetinib (Fig.5C). Next, we assessed the effect of a *USP10* catalytically dead mutant on cell migration. While re-introduction of wt *USP10* into *USP10* depleted cells was shown to suppress cell migration, this was not observed for the catalytically dead *USP10* mutant. Together, these results suggest that USP10 can edit ZEB1 ubiquitination and thereby, influence CRC cell migration through its DUB activity.

ERK phosphorylates USP10 at S236 and promotes its disassociation from ZEB1

We determined whether the interaction of USP10 with ZEB1 is altered by MEK-ERK signaling. We found that the USP10-ZEB1 interaction was attenuated in MEK-ERK activated $BRAF^{V600E}$ compared to *BRAF* wt cells (Fig.6A), and this interaction was enhanced by treatment with cobimetinib (Fig.6B). Since ERK kinases have various cytosolic and nuclear substrates in contrast to RAF and MEK1/2 kinases that have narrow substrate specificity [27], we hypothesized that ERK can phosphorylate USP10 which may alter its interaction with ZEB1. ERK activated $BRAF^{V600E}$ cells showed enhanced phosphorylation of USP10 compared to wt cells (Fig.6C), and suppression of MEK-ERK attenuated USP10 phosphorylation shown to enhance the USP10-ZEB1 interaction (Fig.6D). Analysis of the USP10 protein sequence identified two potential ERK phosphorylation sites, T74 and S236, based on the ERK substrate motif. Whereas mutation

of Thr to Ala at 74 had no effect phosphorylation of USP10 and its interaction with ZEB1, mutation of Ser to Ala at 236 suppressed ERK-mediated USP10 phosphorylation and enhanced the USP10-ZEB1 interaction. Furthermore, treatment of cells expressing this phosphorylation mutant (S236A) with cobimetinib did not alter the phosphorylation event nor the interaction between USP10 and ZEB1 (Fig.6E), and a double mutant behaved similarly to the S236A mutant (Fig.6E). Importantly, expression of the USP10 S236A mutant was shown to suppress K27 ubiquitination and to increase K48 ubiquitination of ZEB1 (Fig.6F) that resulted in its degradation (Fig. 6G) and its suppression of cell migration. Lastly, inhibition of MEK/ERK failed to impact ZEB1 ubiquitination pattern, protein stability and cell migration in cells expressing the S236A mutant (Fig.6F-H).

Targeting MEK-ERK-USP10-ZEB1 axis inhibits metastasis *in vivo*.

To further study the role of the MEK-ERK-USP10- ZEB1 axis in tumor metastasis, we utilized a human-mouse xenograft model. We found that knockdown of *USP10* in RKO cells xenografted into mice promoted lung metastasis to a significantly greater extent compared to xenografted control cells (Fig. 7A,B). Furthermore, knockdown of *ZEB1* was also shown to dramatically suppress lung tumor development, whereas knockdown of *USP10* in *ZEB1*-depleted cells failed to further reduce the number of lung nodules (Fig.7A,B). These results demonstrate that USP10 can regulate CRC cell metastasis through the EMT transcription factor ZEB1.

We then determined whether inhibition of MEK-ERK signaling can suppress tumor metastasis through the USP10-ZEB1 axis in our CRC mouse model. We treated cells with encorafenib in combination with cetuximab since this EGFR inhibitor is needed due to rebound activation of EGRF signaling when RAF/RAS MEK-ERK signaling is inhibited [28]. While treatment with encorafenib or cetuximab alone did not significantly suppressed tumor metastasis, we found that their combination significantly suppressed lung metastasis in our CRC murine model (Fig.7C,D). To further demonstrate the role of USP10 in MEK-ERK-mediated CRC metastasis, we performed knockdown of *USP10* in xenografted CRC cells which was shown to markedly enhance lung metastasis in the presence or absence of treatment with encorafenib, cetuximab or their combination (Fig.7C,D).

Discussion

ZEB1 is a transcription factor that promotes tumor invasion and metastasis via EMT, and its expression increases during neoplastic progression [29]. Among the EMT master transcription factors, only ZEB1 was found to be regulated by the RAS/RAF/MEK/ERK signaling pathway in this study. Constitutive activation of MEK-ERK was shown to stabilize ZEB1 protein, and inhibitors of this signaling pathway suppressed ZEB1 due to a shortened half-life. Posttranslational modifications (PTMs) of ZEB1 regulate protein half-life, sub-cellular localization, and DNA/protein binding ability [30]. To date, few studies have focused on PTMs of ZEB1 which may be critical to its ability to promote tumor metastasis. In this report, we made the novel observation that ERK kinase can phosphorylate USP10 at serine 236 which was

potently suppressed by MEK-ERK inhibition. These events lead to enhanced CRC cell migration and tumor metastasis *in vivo* consistent with the function of ZEB1 as a regulator of EMT and CRC metastasis.

ZEB1 protein is subject to ubiquitination and degradation, however, the specific mechanism by which cellular ZEB1 is stabilized remains unclear. We mutated the ERK-regulated phosphorylation site on USP10 which changed serine to alanine at residue Ser 236 and was shown to impair the dissociation of ZEB1 from its novel interaction with the DUB USP10. ZEB1 has been reported to interact with USP51 resulting in its deubiquitination and stabilization, which is distinct from its deubiquitination by USP10 shown here which resulted in ZEB1 proteasomal degradation [31]. Ubiquitination is achieved through ubiquitin-activating (E1) and -conjugating enzymes (E2) as well as ubiquitin-protein ligase (E3) resulting in ubiquitin being conjugated to a substrate protein. Lysine 48-linked chains and Lysine 63-linked chains are the most well characterized linkages. Importantly, the E3 ligases SIAH1, TRIM26 and FBXO45 are responsible for k48 polyubiquitinated ZEB1 and in this manner, promote ZEB1 degradation. However, the mechanism and function of the atypical lysine 27-linked chains is poorly understood. Lysine 27-linked chains were initially found to localize on the lysosome with a role in mitochondrial autophagy and more recently, were reported to regulate the DNA damage response and autoimmunity. In this study, we identified a novel function of K27-linkage polyubiquitination chains shown to modulate ZEB1 protein stability. To date, only three DUBs have been shown to remove K27-linkage polyubiquitination chains from their substrates. USP19 deubiquitinates the K27-linked chain from TRIF and modulates TLR3/4 innate immune responses[15, 16]. OTUD6A erases K27-linked polyubiquitination of Brg1, and USP38 deposes IL-33 mediated K27-linked ubiquitination of IL-33R to fine tune its activation[15–17]. Here, we found that the DUB activity of USP10 can remove the K27-linked ubiquitin chain from ZEB1 with a resultant increase in K48-linked ubiquitinated ZEB1 that led to its proteasomal degradation. Other examples exist for fine tuning of protein stability by competition with different polyubiquitinated chains. In this regard, K33-linked polyubiquitin chains on TBK1 can prevent its degradation, and USP38 cleaves K33 ubiquitination chains allowing for subsequent K48-linked ubiquitination mediated by DTX4 and TRIP[32]. Understanding the mechanisms that regulate ZEB1 ubiquitination levels may provide a promising strategy for targeting E3 ubiquitin ligase and DUBs in cancer treatment. Two known E3 ligases responsible for K27-linked ubiquitination have been reported, including NEDD4 and HACE1 [33, 34]. Our planned studies will explore whether these or other E3 ligases can contribute to the K27-linked ubiquitination of ZEB1.

We further studied the role of the MEK-ERK-USP10-ZEB1 axis in tumor metastasis using a mouse xenograft model. We found that USP10 can regulate human CRC cell metastasis in this model through ZEB1. Furthermore, inhibition of MEK-ERK signaling was shown to suppress tumor metastasis through the USP10-ZEB1 axis. In human CRCs, mutations in RAS/RAF are key drivers of MEK-ERK signaling and in patients whose CRC harbors a $BRAF^{V600E}$ mutation, treatment with encorafenib combined with the anti-EGFR antibody cetuximab has been shown to extend patient survival and is a standard regimen for this molecularly-defined tumor subset [35]. While treatment with encorafenib or cetuximab alone did not significantly suppressed tumor metastasis in our xenograft model generated using control CRC cells,

whereas the drug combination did achieve suppression of lung metastases. Moreover, suppression of *USP10* was shown to enhance lung tumor metastasis despite treatment with these drugs alone or in combination indicative of drug resistance.

In summary, constitutive activation of MEK-ERK can phosphorylate USP10 at a novel site (S320) shown to disassociate USP10 from ZEB1 that resulted in ZEB1 protein stabilization, enhanced cell migration, and tumor metastasis. Inhibition of MEK-ERK signaling suppressed USP10 phosphorylation, enhanced its interaction with ZEB1, and removed its K27polyubiquitination chain that led to increased K48-linked polyubiquitination and its proteasomal degradation (*shown schematically in* Fig. 8). These events served to suppress ZEB1-regulated EMT and tumor metastasis. Taken together, these findings demonstrate a novel function of USP10 in the regulation of ZEB1 ubiquitination and protein stability that can inhibit ZEB1-mediated tumor metastasis.

Materials & Methods

Cell culture and reagents

Human CRC cell line RKO (ATCC CRL-2577) was obtained from the ATCC (Manassas, Virginia); Colo320 was a gift from Dr. Johnsen (Mayo Clinic). RPMI medium supplemented with 10% (v/v) fetal bovine serum (FBS) were used for culturing CRC cell lines. Dulbecco's modified Eagle's medium supplemented with 10% FBS was used for culturing HEK293T cells. All cell lines were authenticated by short tandem repeat analysis and routinely tested using MycoAlert Mycoplasma detection set. Cells were treated with the following drugs: cobimetinib (GDC-0973/XL-518; Active Biochem, Hongkong, China), BRAF inhibitor vemurafenib (PLX-4032; Active Biochem), cetuximab (Eli Lilly, Indianapolis, Indiana), encorafenib (Selleckchem, Radnor, Pennsylvania) and trametinib (Selleckchem). The following antibodies were used in this study: Snail antibody (Cell Signaling Technology, Danvers, Massachusetts, Cat# 4223), Slug antibody (Cell Signaling Technology Cat# 94296), β tubulin antibody (Cell Signaling Technology Cat# 2146), phospho-p44/42 MAPK (Erk1/2) [Thr202/Tyr204] antibody (Cell Signaling Technology Cat# 4370), p44/42 MAPK (Erk1/2) antibody (Cell Signaling Technology Cat# 4695), E cadherin antibody (Cell Signaling Technology Cat# 3195), ZEB1 antibody for immunoblotting (Bethyl Laboratories, Montgomery, Texas, Cat# A301-922A), ZEB antibody for immunoprecipitation (Santa Cruz Biotechnology, Dallas, Texas, Cat# sc-515797), USP10 antibody for immunoprecipitation (Santa Cruz Biotechnology, Cat# sc-365828), Twist1 antibody (Abcam, Bradford, Massachusetts, Cat#ab50887), K48 linkage ubiquitination antibody (Abcam Cat# ab140601) and K27 linkage ubiquitination antibody (Abcam Cat# ab181537), anti-HA antibody (Proteintech, Rosemont, Illinois, Cat# 51064-2-AP) and Twist2 antibody (Proteintech Cat# 11752-1-AP).

Lentiviral shRNA mediated knockdown

Two Human *USP10* shRNA were transfected with pMD2G (Addgene, Watertown, Massachusetts, Plasmid #12259) and pSPAX2 (Addgene Plasmid #12260) into HEK293T cells to generate lentivirus as previously described [22]. CRC cells were incubated with lentiviruses and 8 μg/ml polybrene per the manufacturer's

instructions. When cells achieved 80% confluence after lentivirus infection, cells were incubated with medium containing puromycin (1:5000 v/v). Forty-eight hours later, knockdown efficiency was determined by immunoblotting. Production and transduction of lentivirus into target cells and elimination of non-transduced target cells were performed per standard procedures, as described previously [24].

Immunoblotting and immunoprecipitation

Immunoblot and immunoprecipitation assays were performed as described previously [25]. Briefly, NETN buffer [20 mM Tris-HCl (pH 8.0), 1 mM EDTA, 0.5% Nonidet P-40, 100 mM NaCl], 10 mM NaF, 50 mM β-glycerophosphate, and 1 mg/ ml each of pepstatin A and aprotinin were used to lyze the cells. Cell lysates were centrifuged at 10,000 rpm for 15 min and the supernatant was removed and incubated with 2 μg of the indicated antibody and 20 μl protein A or protein G Sepharose beads (GE Healthcare, Marlborough, Massachusetts) overnight at 4°C. Immunoprecipitates were centrifuged at 8000 rpm for 1 min, washed twice with cold NETN buffer and boiled with 1× Laemmli buffer for 10 min. The samples were separated by SDS–PAGE and then transferred to PVDF membranes using the semi-dry method (Trans-Blot® Turbo™ Transfer System, Bio-Rad, Hercules, California). PVDF membranes were incubated with 5% milk for 1 h, following by incubation with the indicated primary antibody overnight at 4^{o}C. On the following day, the membrane was washed with PBST buffer x3, and then incubated with goat anti-rabbit HRP (Jackson Immunoresearch, West Grove, Pennsylvania, AB_2313567) or goat anti-mouse HRP (Jackson Immunoresearch, AB_10015289) secondary antibodies for 1 hour. After washing x3 in PBST buffer, the membranes were incubated with ECL and the signal was detected by Azure Imaging system (Dublin, California) or X-ray film.

Deubiquitination assay

Deubiquitination assays were performed as previously described [22]. Briefly, cells with the indicated treatments were incubated with 10μM MG132 for 6 hours. Cells were then lysed using 1% SDS, boiled at 100^{o} C for 20 min, and diluted with NETN buffer containing a protease inhibitor cocktail. The cell lysate supernatant was immunoprecipitated with ZEB1 antibody and the immunocomplexes were analyzed by immunoblot assay.

Wound healing assay

A wound healing assay was performed as previously described [26]. RKO cells were seeded in 6-well plates and cultured in RPMI1640 media containing 10% FBS until 100% confluence was achieved at which time, media was replaced with serum-free medium and incubated for 24 hours. Monolayer cells were scraped off with a P200 tip and washed several times to remove cellular debris. Cells were then cultured with complete medium in the presence of mitomycin C (10μg/mL), to block cell proliferation, in addition to the indicated treatment. After 16 hours, cells were fixed with 3.7% paraformaldehyde and images were acquired.

Transwell assay

To assess cell migration, RKO cells in serum free RPMI media with the indicated treatments were placed in the top chamber of transwell migration chambers (8.0 μm pore polycarbonate membrane insert; Corning, Glendale, Arizona). The lower wells were filled with RPMI supplemented with 10% FBS and the indicated treatment. Twenty-four hours later, cells were removed from the top surface of the transwell membrane using a cotton swab and migrated cells on the lower membrane surface were fixed, stained, photographed, and counted at light microscopy 20X magnification.

Animal studies

All animal experiments were performed following the protocol approved by the Institutional Animal Care and Use Committee (Mayo Clinic, Rochester, Minnesota). Female 4–6 weeks old Balb/c nude mice (strain #:002019) were purchased from Jackson Laboratory. For analyzing lung metastasis, 1×10^6 RKO parental cells or knockdown cells were resuspended in sterile PBS and injected into the lateral tail vein of the nude mice. After 7 days of injection, mice were randomized into control or treatment groups (n = 5) and treated with indicated drugs either by gavage feeding or by i.p. injection until termination of the experiment. Mice were euthanized at week 10 and visible lung metastatic nodules were examined using a dissecting microscope. Quantification and data analysis were performed blinded to treatment arms.

Statistical analysis

Data derived from the transwell assay and the tail vein injection assay were presented as mean ± standard deviation (SD) or standard error of the mean (SEM). All cell culture experiments were performed in triplicate. Data were analyzed using the Student's t test (two-tailed) or one way ANOVA as indicated, and results were considered statistically significant if $*p < 0.05$ or $**p < 0.01$, as shown.

Declarations

Data availability

All data generated or analyzed during this study are available within the article or available from the authors upon request.

ACKNOWLEDGEMENTS

This study was supported, in part, by NCI R01 CA210509-01A1 and Mayo Clinic Center for Biomedical Discovery Pilot Grant Program (both to FAS). LS is supported by the Second Affiliated Hospital of Guangzhou Medical University, Guangzhou, China.

AUTHOR CONTRIBUTIONS

FS and BQ designed the experiments, BQ, LS and JY performed the experiments, LS, BQ, and FS analyzed and interpreted the study data. BQ and FS wrote the paper that was reviewed by all authors.

COMPETING INTERESTS

The authors declare no competing interests.

References

1. Siegel RL, Miller KD, Fuchs HE, Jemal A. Cancer Statistics, 2021. *CA Cancer J Clin* 2021; 71: 7–33.
2. Biller LH, Schrag D. Diagnosis and Treatment of Metastatic Colorectal Cancer: A Review. JAMA 2021; 325: 669–685.
3. Mittal V. Epithelial Mesenchymal Transition in Tumor Metastasis. Annu Rev Pathol 2018; 13: 395–412.
4. De Craene B, Berx G. Regulatory networks defining EMT during cancer initiation and progression. Nat Rev Cancer 2013; 13: 97–110.
5. Ribatti D, Tamma R, Annese T. Epithelial-Mesenchymal Transition in Cancer: A Historical Overview. Transl Oncol 2020; 13: 100773.
6. Karihtala P, Auvinen P, Kauppila S, Haapasaari KM, Jukkola-Vuorinen A, Soini Y. Vimentin, zeb1 and Sip1 are up-regulated in triple-negative and basal-like breast cancers: association with an aggressive tumour phenotype. Breast Cancer Res Treat 2013; 138: 81–90.
7. Liu Y, Lu X, Huang L, Wang W, Jiang G, Dean KC *et al*. Different thresholds of ZEB1 are required for Ras-mediated tumour initiation and metastasis. Nat Commun 2014; 5: 5660.
8. Manshouri R, Coyaud E, Kundu ST, Peng DH, Stratton SA, Alton K *et al*. ZEB1/NuRD complex suppresses TBC1D2b to stimulate E-cadherin internalization and promote metastasis in lung cancer. Nat Commun 2019; 10: 5125.
9. Sanchez-Tillo E, Lazaro A, Torrent R, Cuatrecasas M, Vaquero EC, Castells A *et al*. ZEB1 represses E-cadherin and induces an EMT by recruiting the SWI/SNF chromatin-remodeling protein BRG1. Oncogene 2010; 29: 3490–3500.
10. Lindner P, Paul S, Eckstein M, Hampel C, Muenzner JK, Erlenbach-Wuensch K *et al*. EMT transcription factor ZEB1 alters the epigenetic landscape of colorectal cancer cells. Cell Death Dis 2020; 11: 147.
11. Chen A, Wong CS, Liu MC, House CM, Sceneay J, Bowtell DD *et al*. The ubiquitin ligase Siah is a novel regulator of Zeb1 in breast cancer. Oncotarget 2015; 6: 862–873.
12. Xu M, Zhu C, Zhao X, Chen C, Zhang H, Yuan H *et al*. Atypical ubiquitin E3 ligase complex Skp1-Pam-Fbxo45 controls the core epithelial-to-mesenchymal transition-inducing transcription factors. Oncotarget 2015; 6: 979–994.
13. Hershko A, Ciechanover A. The ubiquitin system. Annu Rev Biochem 1998; 67: 425–479.
14. Akutsu M, Dikic I, Bremm A. Ubiquitin chain diversity at a glance. J Cell Sci 2016; 129: 875–880.
15. Wu X, Lei C, Xia T, Zhong X, Yang Q, Shu HB. Regulation of TRIF-mediated innate immune response by K27-linked polyubiquitination and deubiquitination. Nat Commun 2019; 10: 4115.

16. Fu X, Zhao J, Yu G, Zhang X, Sun J, Li L *et al*. OTUD6A promotes prostate tumorigenesis via deubiquitinating Brg1 and AR. Commun Biol 2022; 5: 182.
17. Yi XM, Li M, Chen YD, Shu HB, Li S. Reciprocal regulation of IL-33 receptor-mediated inflammatory response and pulmonary fibrosis by TRAF6 and USP38. Proc Natl Acad Sci U S A 2022; 119: e2116279119.
18. Soncini C, Berdo I, Draetta G. Ras-GAP SH3 domain binding protein (G3BP) is a modulator of USP10, a novel human ubiquitin specific protease. Oncogene 2001; 20: 3869–3879.
19. Yuan J, Luo K, Zhang L, Cheville JC, Lou Z. USP10 regulates p53 localization and stability by deubiquitinating p53. Cell 2010; 140: 384–396.
20. Lim R, Sugino T, Nolte H, Andrade J, Zimmermann B, Shi C *et al*. Deubiquitinase USP10 regulates Notch signaling in the endothelium. Science 2019; 364: 188–193.
21. Lin Z, Yang H, Tan C, Li J, Liu Z, Quan Q *et al*. USP10 antagonizes c-Myc transcriptional activation through SIRT6 stabilization to suppress tumor formation. Cell Rep 2013; 5: 1639–1649.
22. Deng M, Yang X, Qin B, Liu T, Zhang H, Guo W *et al*. Deubiquitination and Activation of AMPK by USP10. Mol Cell 2016; 61: 614–624.
23. Sun J, Li T, Zhao Y, Huang L, Sun H, Wu H *et al*. USP10 inhibits lung cancer cell growth and invasion by upregulating PTEN. Mol Cell Biochem 2018; 441: 1–7.
24. Yu J, Qin B, Moyer AM, Nowsheen S, Tu X, Dong H *et al*. Regulation of sister chromatid cohesion by nuclear PD-L1. Cell Res 2020; 30: 590–601.
25. Sun L, Patai AV, Hogenson TL, Fernandez-Zapico ME, Qin B, Sinicrope FA. Irreversible JNK blockade overcomes PD-L1-mediated resistance to chemotherapy in colorectal cancer. Oncogene 2021; 40: 5105–5115.
26. Liu T, Yu J, Deng M, Yin Y, Zhang H, Luo K *et al*. CDK4/6-dependent activation of DUB3 regulates cancer metastasis through SNAIL1. Nat Commun 2017; 8: 13923.
27. Roskoski R, Jr. ERK1/2 MAP kinases: structure, function, and regulation. Pharmacol Res 2012; 66: 105–143.
28. Prahallad A, Sun C, Huang S, Di Nicolantonio F, Salazar R, Zecchin D *et al*. Unresponsiveness of colon cancer to BRAF(V600E) inhibition through feedback activation of EGFR. Nature 2012; 483: 100–103.
29. Drapela S, Bouchal J, Jolly MK, Culig Z, Soucek K. ZEB1: A Critical Regulator of Cell Plasticity, DNA Damage Response, and Therapy Resistance. Front Mol Biosci 2020; 7: 36.
30. Perez-Oquendo M, Gibbons DL. Regulation of ZEB1 Function and Molecular Associations in Tumor Progression and Metastasis. Cancers (Basel) 2022; 14.
31. Zhou Z, Zhang P, Hu X, Kim J, Yao F, Xiao Z *et al*. USP51 promotes deubiquitination and stabilization of ZEB1. Am J Cancer Res 2017; 7: 2020–2031.
32. Lin M, Zhao Z, Yang Z, Meng Q, Tan P, Xie W *et al*. USP38 Inhibits Type I Interferon Signaling by Editing TBK1 Ubiquitination through NLRP4 Signalosome. Mol Cell 2016; 64: 267–281.

33. Pei G, Buijze H, Liu H, Moura-Alves P, Goosmann C, Brinkmann V *et al*. The E3 ubiquitin ligase NEDD4 enhances killing of membrane-perturbing intracellular bacteria by promoting autophagy. Autophagy 2017; 13: 2041–2055.
34. Palicharla VR, Maddika S. HACE1 mediated K27 ubiquitin linkage leads to YB-1 protein secretion. Cell Signal 2015; 27: 2355–2362.
35. Tabernero J, Grothey A, Van Cutsem E, Yaeger R, Wasan H, Yoshino T *et al*. Encorafenib Plus Cetuximab as a New Standard of Care for Previously Treated BRAF V600E-Mutant Metastatic Colorectal Cancer: Updated Survival Results and Subgroup Analyses from the BEACON Study. J Clin Oncol 2021; 39: 273–284.

Figures

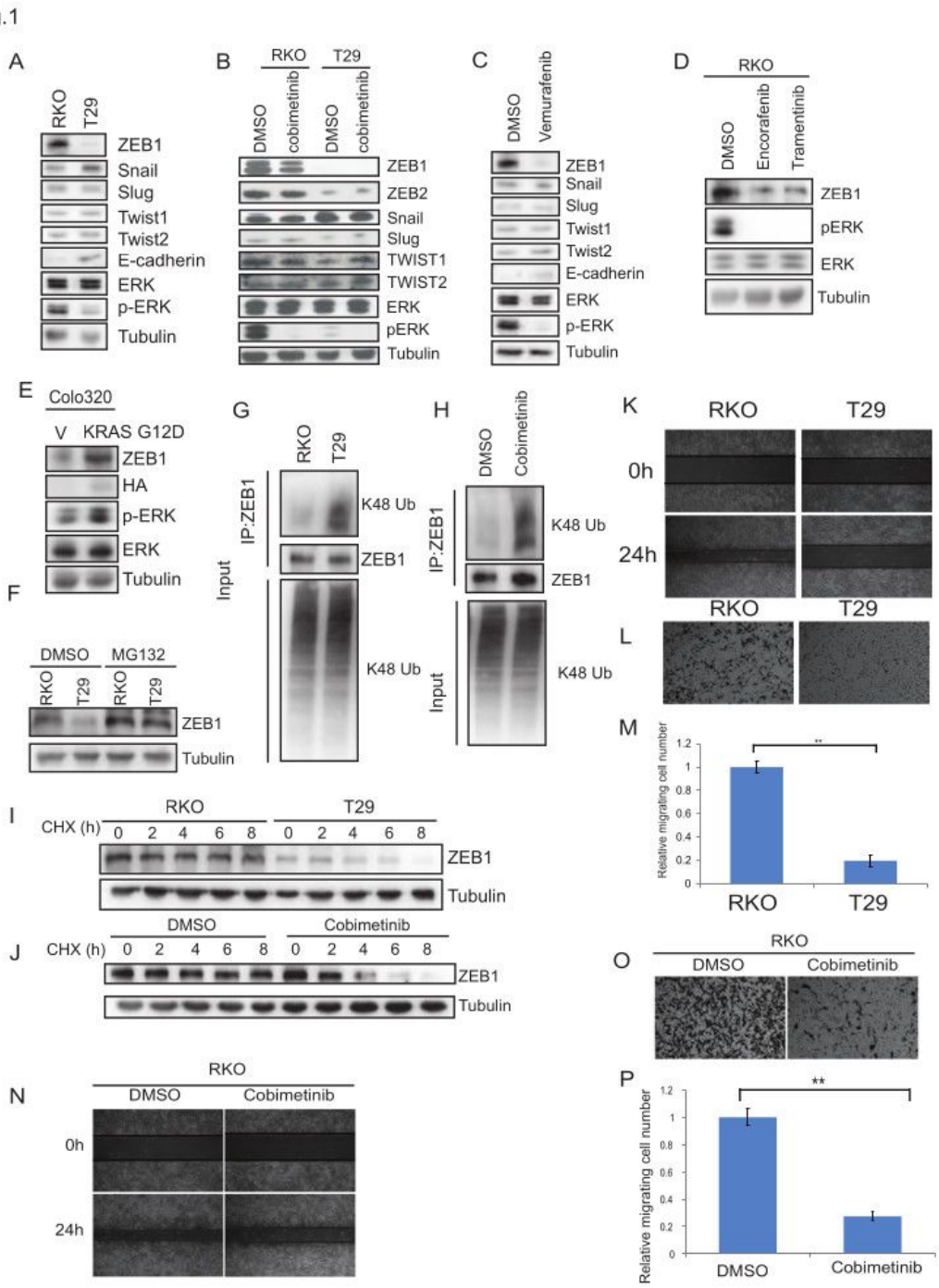

Figure 1

MEK-ERK signaling regulates ZEB1 protein stability and CRC cell migration.

A, Immunoblot analysis of expression of EMT master transcription factors in isogenic RKO cells including parental RKO (*BRAF*$^{V600E/V600E/wt}$) and T29 (*BRAF*$^{wt/-/-}$). **B,** Immunoblotting of EMT factors in isogenic RKO cells treated with vehicle or MEK inhibitor, cobimetinib (2μM). **C,** Immunoblotting of EMT factor

proteins in RKO cells treated with BRAF inhibitor vemurafenib (5μM) or vehicle. **D-E,** Detection of ZEB1 protein expression in RKO cells treated with the *BRAF*^{V600E} inhibitor, encorafinib combined with the MEK inhibitor, trametinib (10μM) (**D**), and Colo320 cells transfected with *KRAS G12D* (**E**). **G-H,** Analysis of K48 linkage polyubiquitination of ZEB1 in isogenic RKO cells (**G**) and RKO cells treated with vehicle or cobimetinib (2μM) (**H**). **I-J,** Determination of ZEB1 protein half-life in isogenic RKO cells (**I**) and RKO cells treated with vehicle or cobimetinib (**J**). **K-L** Analysis of isogenic RKO cell migration in wound healing (**K**) and transwell (**L**) assays. **M** Quantification of migrated cells shown in (**L**). **N-O** Analysis of RKO cell migration in presence of cobimetinib (2μM) or vehicle by wound healing (**N**) and transwell (**O**) assays. **P** Quantification of migrated cells in (**O**). Migrated cells were quantified from images (n=5) (**M,P**). Data are presented as mean ± SD. Student t test. **, $p < 0.01$.

Fig.2

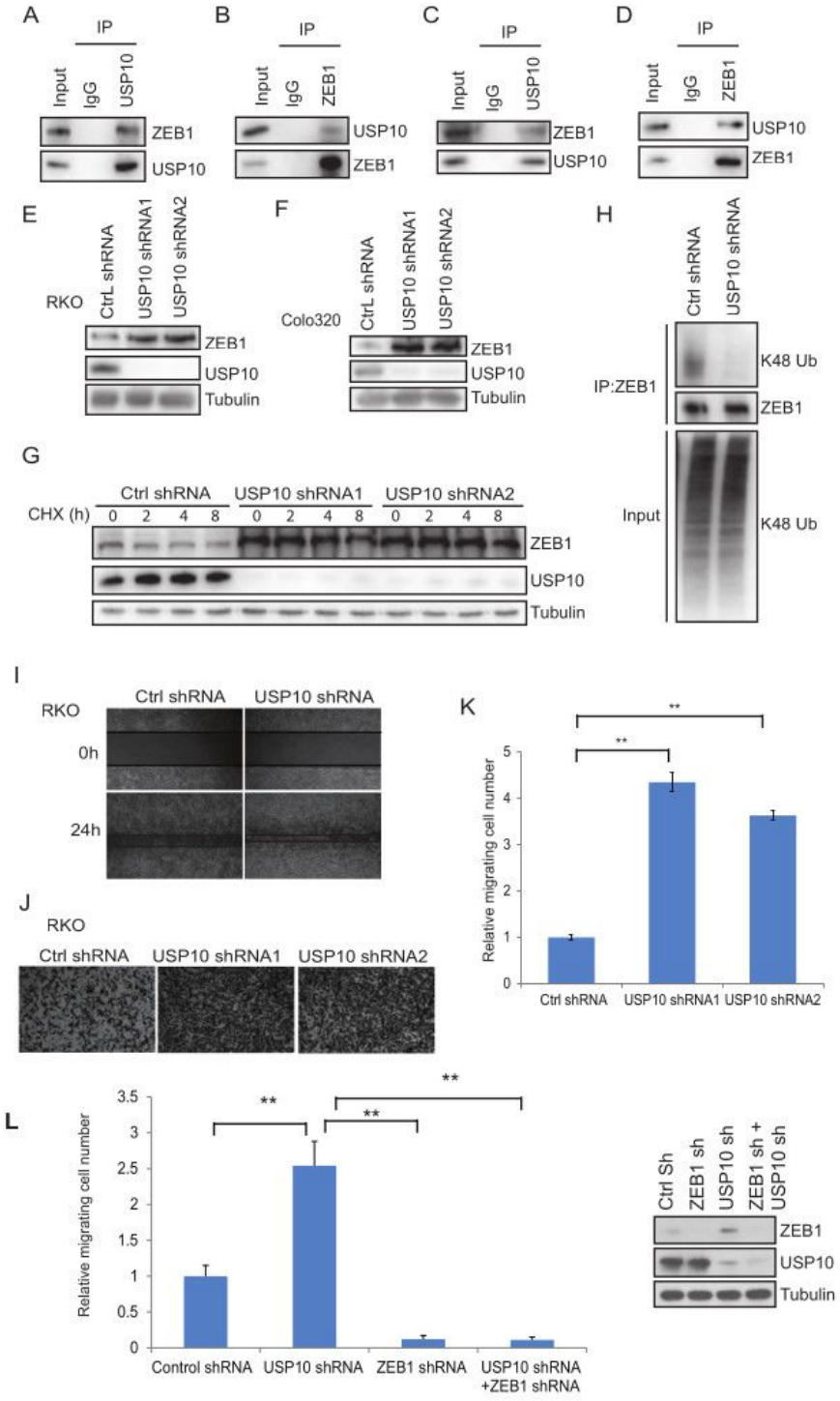

Figure 2

USP10 interacts with and stabilizes ZEB1 leading to suppression of CRC cell migration.

A-D, Interaction of ZEB1 and USP10 by immunoprecipitation in RKO (**A-B**) or Colo320 cells (**C-D**). **E-F,** Immunoblotting of ZEB1 in control shRNA and two different *USP10* shRNA-expressing RKO (**E**) or Colo320 cell lines (**F**). **G,** Analysis of K48 linkage polyubiquitination of ZEB1 in *USP10* knockdown cells vs

control cells. **H,** Determination of ZEB1 protein half-life in control shRNA or *USP10* shRNA expressing cells. **I-J,** Analysis of cell migration by wound healing assay in RKO cells expressing control shRNA or *USP10* shRNA (**I**) and also shown in a transwell assay (**J**). **K,** Quantification of migrated cells in (**J**). **L** ,Quantification cell migration by transwell assay in RKO cells expressing control shRNA, *USP10* shRNA, *ZEB1* shRNA or *USP10 shRNA/ZEB1 shRNA*. Migrated cells were quantified from the images (n=5) (**K,L**). Data are presented as mean ±SEM one-way ANOVA t-test. **, $p < 0.01$.

Fig.3

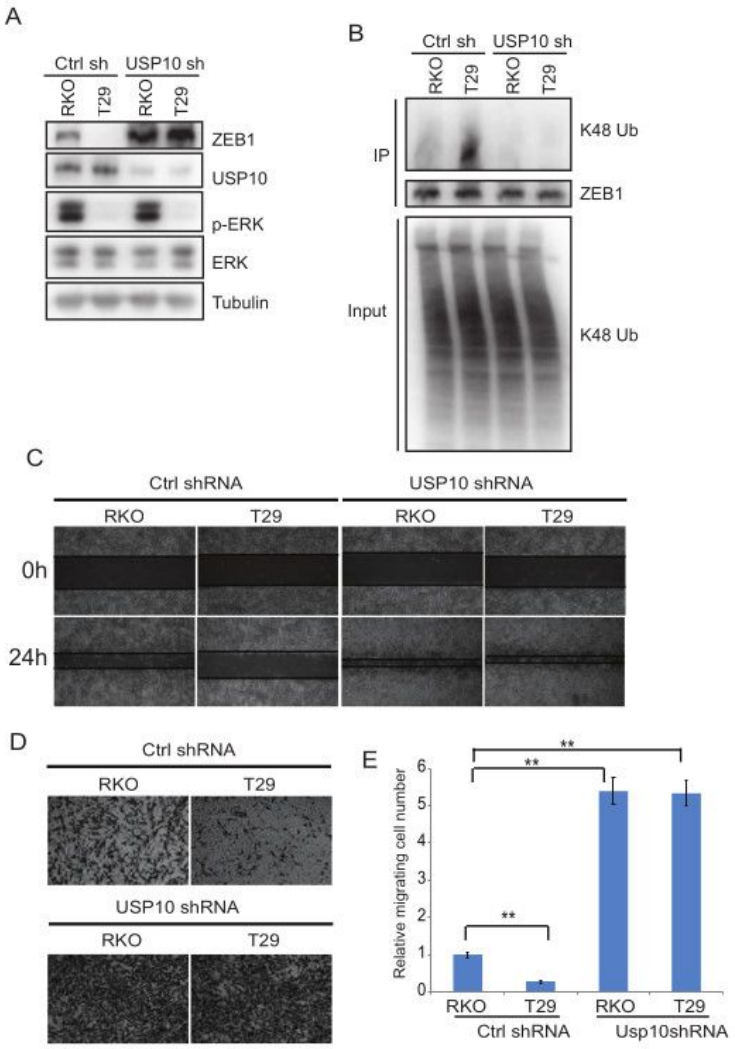

Figure 3

Constitutive activation of MEK-ERK signaling stabilizes ZEB1 through USP10.

A, Analysis of ZEB1 protein expression in isogenic RKO cells expressing control shRNA or *USP10* shRNA. **B,** Immunoblotting of K48 linkage polyubiquitination of ZEB1 in control shRNA- or *USP10* shRNA-expressing isogenic RKO cells. **C-D,** Assessment of cell migration by wound healing assay in isogenic

RKO cells expressing control shRNA or *USP10* shRNA (**C**) and transwell assay (**D**). **E,** Quantification of migrated cells in (**D**). Migrated cells were quantified from the images (n=5) (**E**). Data are presented as mean ±SEM one-way ANOVA t-test . **, p < 0.01.

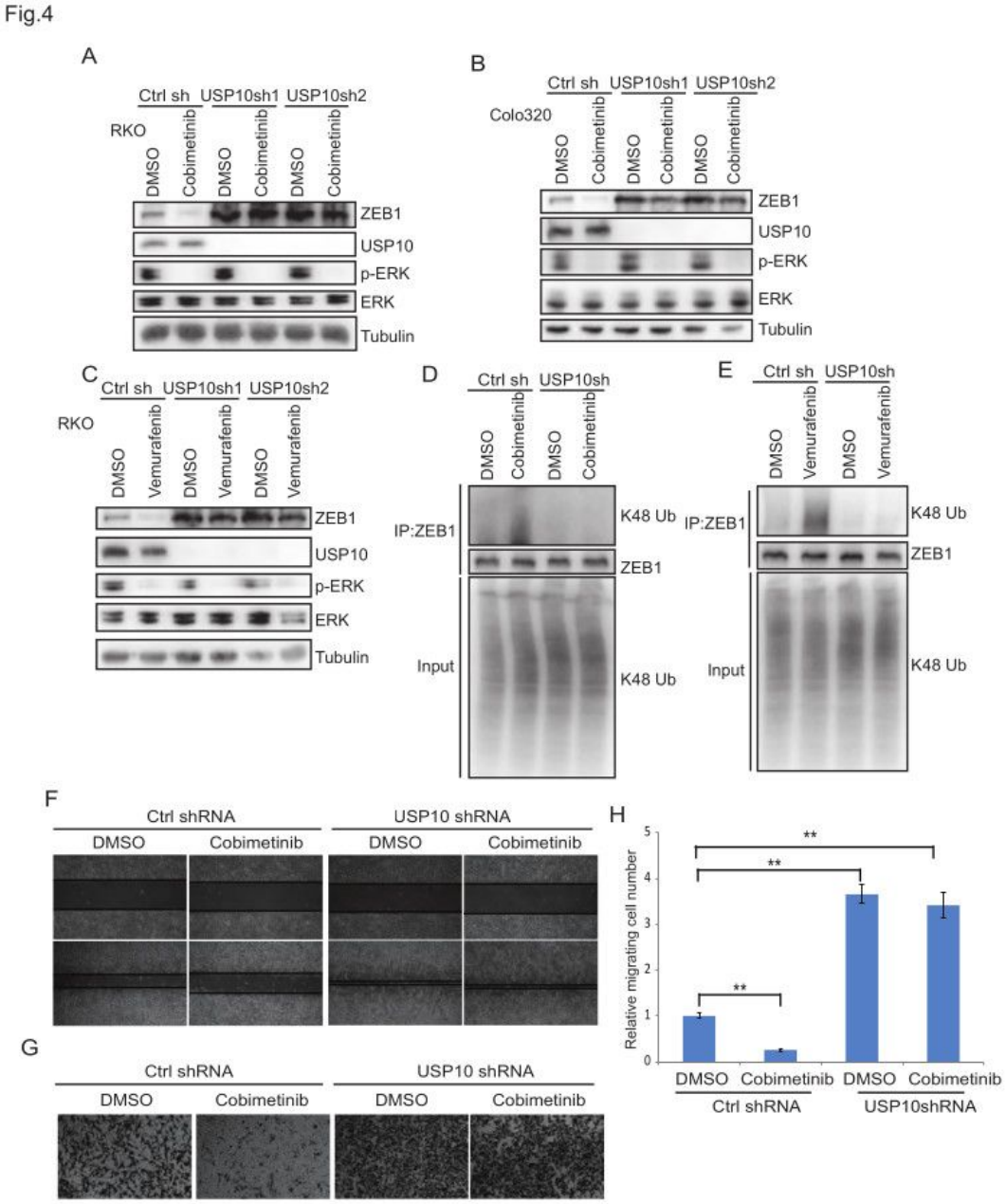

Figure 4

Targeting MEK-ERK signaling destabilizes ZEB1 through USP10.

A-B, Immunoblot showing ZEB1 protein expression in control shRNA or two different *USP10* shRNA expressing RKO cells (**A**)or Colo320 cells (**B**) with or without treatment with cobimetinib.

C, Immunoblot assessment of ZEB1 protein expression in control shRNA or two different *USP10* shRNA expressing RKO cells in presence or absence of vemurafenib. **D-E,** Analysis of K48 linkage polyubiquitination of ZEB1 in RKO cells expressing control shRNA or *USP10* shRNA with or without cobimetinib (**D**) or vemurafenib (**E**). **F-G,** Assessment of cell migration in RKO cells expressing control shRNA or *USP10* shRNA treated with vehicle or cobimetinib in a wound healing assay (**F**) or transwell assay (**G**). **H** Quantification of migrated cells in (**G**). Migrated cells were quantified from the images (n=5) (**H**). Data are presented as mean ±SEM one-way ANOVA t-test. **, $p < 0.01$.

Fig.5

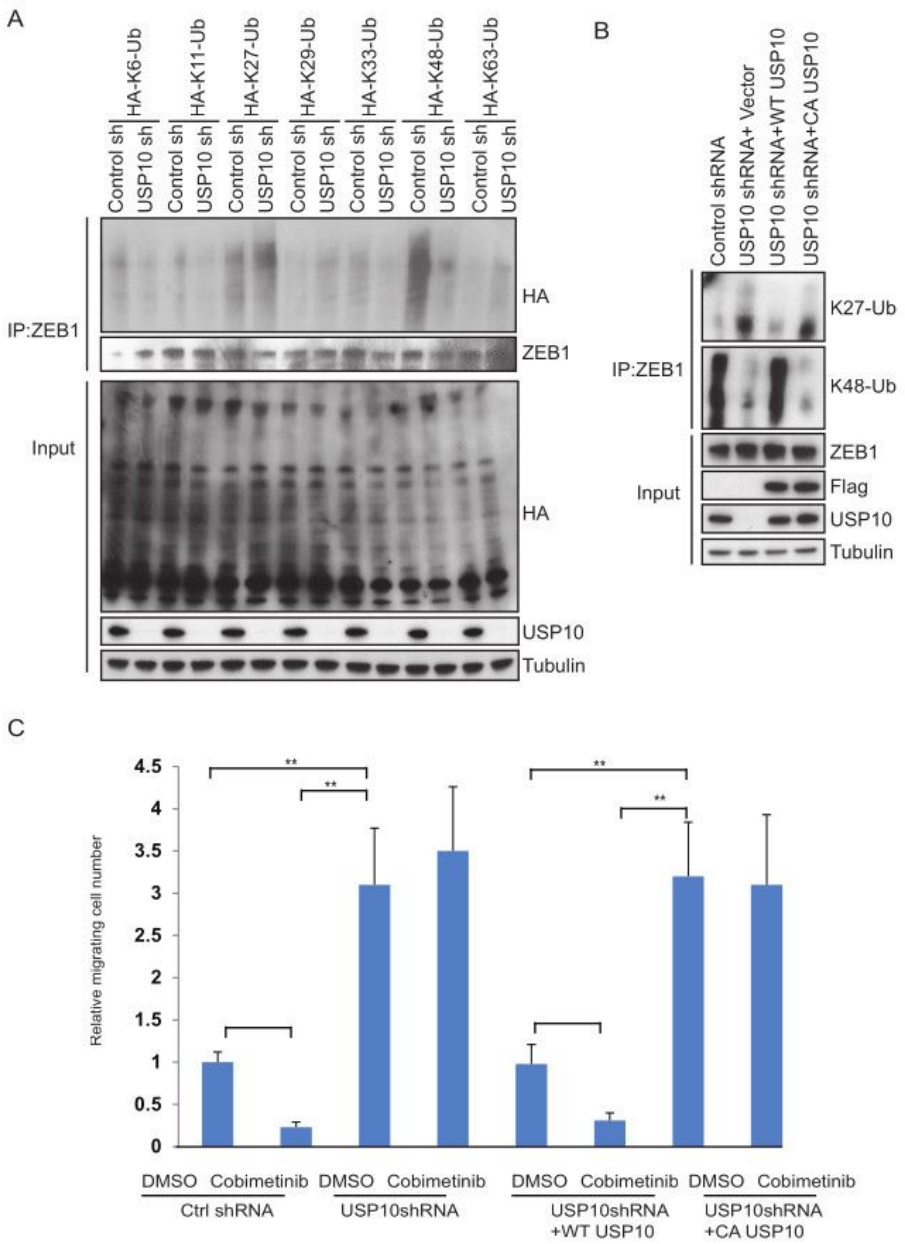

Figure 5

USP10 edits ZEB1 ubiquitination.

A, Analysis of effect of USP10 on ZEB1 ubiquitination using a panel of ubiquitin mutants. **B,** Analysis of ZEB1 K27 linkage and K48 linkage polyubiquitination in RKO cells expressing control shRNA, *USP10* shRNA, wildtype USP10 reconstituted cells or *USP10* catalytically dead mutant cells. **C,** Quantification of

cell migration (transwell assay) in RKO cells expressing control shRNA, *USP10* shRNA, *USP10* shRNA+ WT USP10, and USP10 shRNA+ CA USP10 in presence or absence of cobimetinib. Migrated cells were quantified from the images (n=5) (**C**). Data are presented as mean ±SEM one-way ANOVA t-test. **, $p < 0.01$.

Fig.6

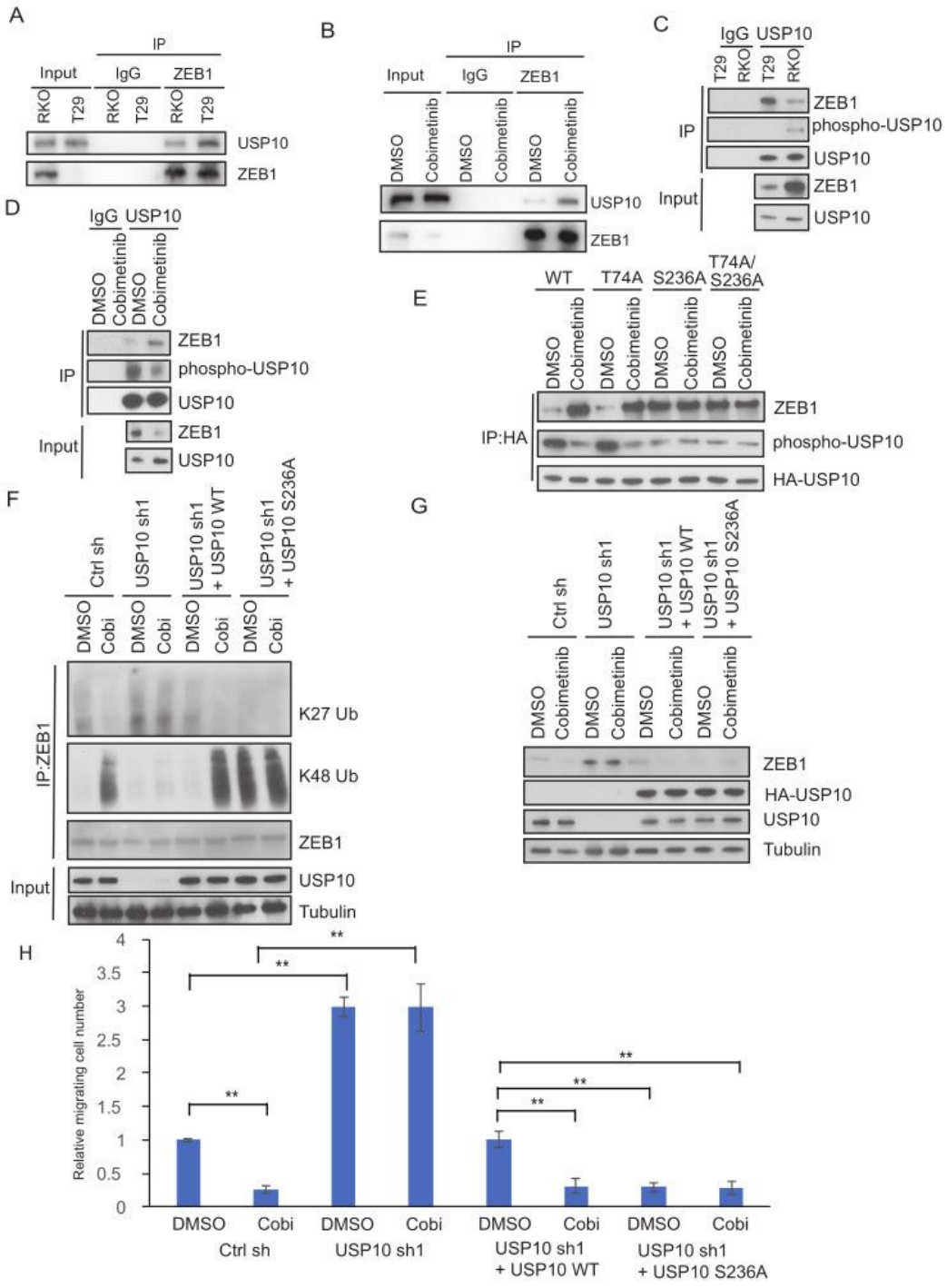

Figure 6

Phosphorylation of USP10 by ERK impairs its interaction with ZEB1 and results in ZEB1 stabilization.

A-D, Analysis of interaction between ZEB1 and USP10 by co-immunoprecipitation in isogenic RKO cells (**A, C**) or RKO cells treated with vehicle or cobimetinib(**B,D**). **E,** Identification of the ERK-mediated phosphorylation site on USP10 protein. Phospho-MAPK substate antibody is used to detect phosphorylation of USP10 by ERK. **F-H,** Analysis of ZEB1 K27 linkage and K48 linkage polyubiquitination (**F**) ZEB1 protein expression (**G**) or cell migration (**H**) in RKO cells expressing control shRNA, *USP10* shRNA, wildtype *USP10* reconstituted cells or *USP10* S236A mutant expressing cells in the presence or absence of cobimetinib treatment. Migrated cells were quantified from the images (n=5) (**H**). Data are presented as mean ±SEM one-way ANOVA t-test. **, $p < 0.01$.

Fig.7

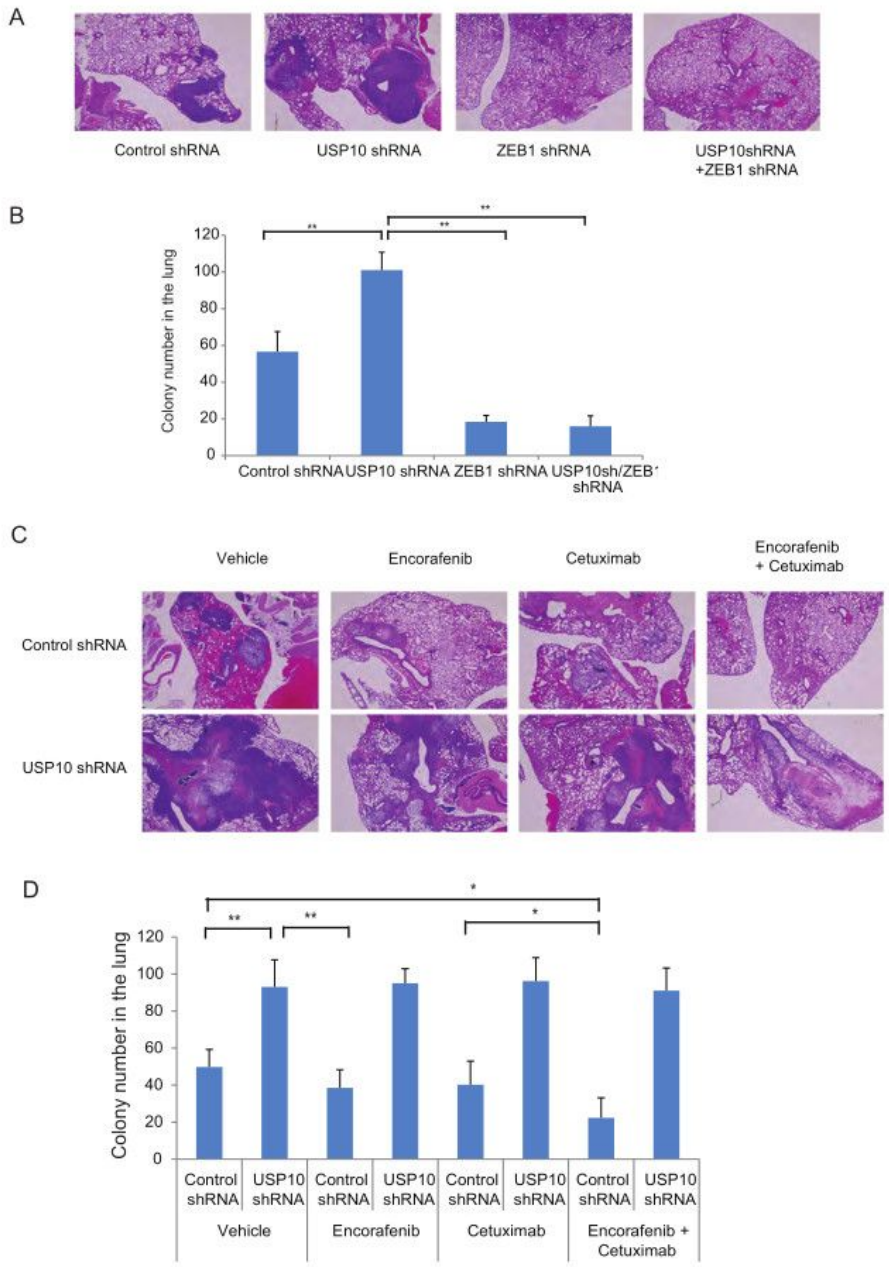

Figure 7

Inhibition of MEK-ERK-USP10-ZEB1 signaling suppresses CRC metastasis *in vivo*.

A, Representative image (H&E sections) of metastatic lung nodules generated by tail vein injection of RKO cells into nude mice. Injected RKO cells included those expressing control shRNA, *USP10* shRNA, *ZEB1* shRNA, and *USP10* shRNA+ ZEB1 shRNA expressing RKO cell. **B,** Quantification of metastatic lung

nodules in (**A**). **C,** Representative image (H&E) of metastatic lung nodules induced by injection of RKO cells expressing control shRNA or *USP10* shRNA in presence of vehicle, encorafenib, cetuximab, or their combination. **D,** Quantification of metastatic lung nodules in (**C**). lung colonies were quantified from the lung tissue (n=5) (**B,D**). Data are presented as mean ±SEM one-way ANOVA t-test. *, $p < 0.05$,**, $p < 0.01$.

Fig.8

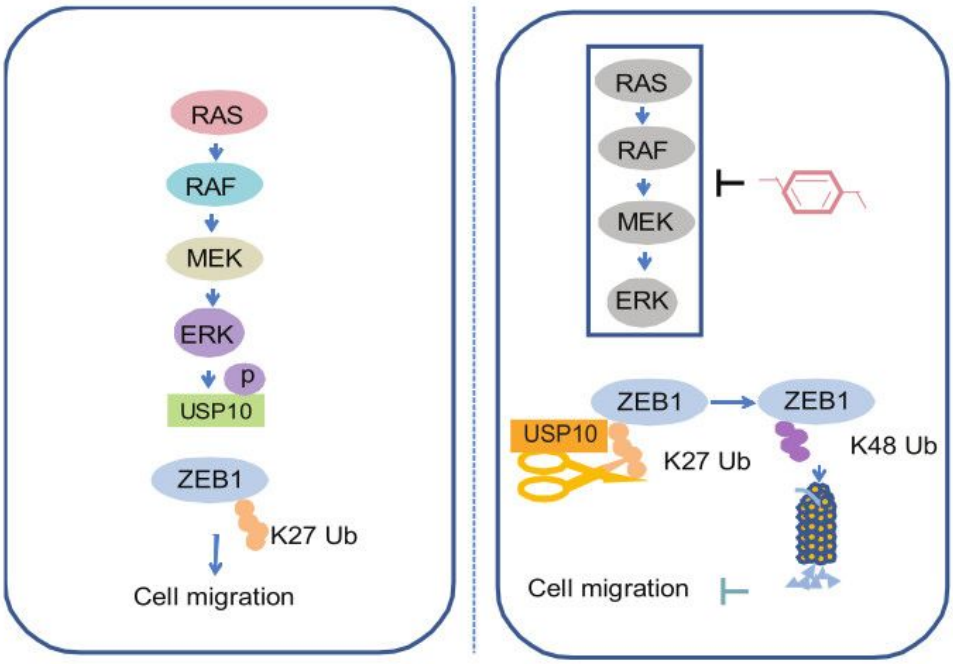

Figure 8

Schematic Model. Constitutive activation of the RAS/RAS/MEK/ERK axis phosphorylates USP10 at S236, and this phosphorylation induces the dissociation of USP10 from ZEB1 resulting in stabilization of ZEB1. These events lead to enhanced cell migration and tumor metastasis (***left panel***). Inhibition of MEK-ERK signaling is shown to suppress ERK-mediated USP10 phosphorylation and increase the USP10-ZEB1 interaction which enhances cleavage of the K27 linkage polyubiquitination chain from ZEB1. K27 polyubiquitin chain cleavage leads to increased K48 linked polyubiquitination of ZEB1 and its proteasomal degradation that can suppress cell migration and metastasis(***right panel***).

Supplementary Files

This is a list of supplementary files associated with this preprint. Click to download.

- TableS1.docx